

The quasi-continuous exhaust regime in ASDEX Upgrade and JET

M. Faitsch ^a,*, M. Dunne ^a, E. Lerche ^{b,c}, P. Lomas ^c, I. Balboa ^c, P. Bilkova ^h, P. Bohm ^h, L. Gil ^f, G.F. Harrer ^g, A. Kappatou ^a, D. Kos ^e, B. Labit ^d, L. Radovanovic ^g, A. Redl ^a, O. Sauter ^d, S. Silburn ^c, E.R. Solano ⁱ, A. Tookey ^c, E. Viezzzer ^e, E. Wolfrum ^a, U. Stroth ^{a,j}, JET contributors¹, the ASDEX Upgrade Team², the EUROfusion Tokamak Exploitation Team³

^a Max-Planck-Institute for Plasma Physics, Boltzmannstr. 2, 85748 Garching, Germany

^b Laboratory for Plasma Physics LPP-ERM/KMS, B-1000 Brussels, Belgium

^c United Kingdom Atomic Energy Authority, Culham Science Centre, Abingdon, Oxon, OX14 3DB, United Kingdom of Great Britain and Northern, Ireland

^d Ecole Polytechnique Federale de Lausanne, Swiss Plasma Center, CH-1015, Lausanne, Switzerland

^e Dept. of Atomic, Molecular and Nuclear Physics, University of Seville, Spain

^f Instituto de Plasmas e Fusão Nuclear, Instituto Superior Técnico, Universidade de Lisboa, 1049-001 Lisboa, Portugal

^g Institute of Applied Physics, TU Wien, Fusion@ÖAW, Wiedner Hauptstr. 8-10, 1040 Vienna, Austria

^h Institute of Plasma Physics of the CAS, Prague, Czech Republic

ⁱ Laboratorio Nacional de Fusión, CIEMAT, Spain

^j Physik Department E28, Technische Universität München, 85748 Garching, Germany

ARTICLE INFO

Keywords:

ELM-free scenario

Type-II ELMs

Quasi-continuous exhaust regime

Power exhaust

Ballooning modes

ABSTRACT

The quasi-continuous exhaust (QCE) regime is a type-I ELM-free high confinement regime obtained at high plasma shaping and high separatrix density. A comparison with various ELM-free regimes in the literature is presented together with potential physics models for accessing the QCE regime. The regime was recently successfully ported from ASDEX Upgrade to JET. We present a first comparison between the achieved plasma conditions in the two tokamaks and an extrapolation towards ITER and EU-DEMO parameters. The step in size from ASDEX Upgrade to JET successfully lowered the pedestal top collisionality, demonstrating that the regime is not limited to high collisionality at the pedestal top but naturally operates at high density. The extrapolation to ITER and EU-DEMO parameters shows that they can reach the conditions in which ASDEX Upgrade and JET are operating in QCE without type-I ELMs applying previously proposed physics models.

1. Introduction

High confinement and edge localised modes (ELMs) are historically linked in tokamak operation. Over the years, different types of ELMs were identified [1], with the large type-I ELMs appearing in the favoured H-mode regime for decades [2]. Only in recent years, alternatives are gaining more focus because it was shown that unmitigated type-I ELMs will lead to unacceptable first wall loading in a reactor [3,4].

Here, we discuss one specific type-I ELM-free regime which is called the quasi-continuous exhaust (QCE) regime [5]. While significant progress in experimental exploitation and theoretical understanding of the regime has been achieved in recent years, some major open

questions remain: (i) What is the role of the pedestal top collisionality which is elevated in the medium sized machines compared to that expected in ITER, (ii) how affect filaments detachment and the first wall energy and particle loads and (iii) is the transport caused by filaments preventing the pedestal from reaching the peeling-ballooning boundary avoiding type-I ELMs.

The paper is organised as follows. We summarised the historical evolution of the regime leading to the re-naming into QCE and the similarities to other type-I ELM-free regimes in Section 2. The physics picture behind the absence of type-I ELMs is highlighted in Section 3. A comparison between ASDEX Upgrade (AUG) and JET together with a first extrapolation to reactor-sized machines, including open questions,

* Corresponding author.

E-mail address: Michael.Faitsch@ipp.mpg.de (M. Faitsch).

¹ See the author list of C. Maggi et al, 2024 Nucl. Fusion <https://doi.org/10.1088/1741-4326/ad3e16>.

² See the author list of H. Zohm et al, 2024 Nucl. Fusion <https://doi.org/10.1088/1741-4326/ad249d>.

³ See the author list of E. Joffrin et al, 2024 Nucl. Fusion <https://doi.org/10.1088/1741-4326/ad2be4>.

is shown in Section 4. The paper finishes with a summary and an outlook in Section 5.

2. The QCE in relation to other similar type-I ELM-free regimes

A variety of similar regimes exist on many tokamaks. The various definitions are presently not strict enough to ultimately distinguish them. An overview of many no- and small-ELM regimes is provided e.g. in [6] and specifically for AUG in table 1 of [7].

The QCE regime comes with high shaping and high fuelling in which type-I ELMs are replaced by low-amplitude, high-frequent transients which we call filaments. These filaments were originally called type-II ELMs in AUG [8–10], JET [11–14] and MAST [15]. The name then evolved to *small ELMs* in AUG [16] and TCV [17] and since 2021 the term *quasi-continuous exhaust regime* is used for the same regime [5,18–27].

The change of name came along with experimental evidence for the origin of the transients. While the earlier work hinted to the pedestal top as origin of the filaments [8], it was later shown that it is the pedestal foot, close to the separatrix [16]. Early models related the transients to the pedestal top collisionality and to a resistive MHD instability [28]. With recent high resolution measurements in the region [16], the physics interpretation changed as well. Now, local ballooning modes located close to the separatrix are proposed as the origin, see Section 3.

This different interpretation has some major implications. The separatrix region in medium sized and reactor grade tokamaks is comparable in terms of density and collisionality, while the parameters at the pedestal top are expected to deviate significantly. Thus, while the older interpretation extrapolated very unfavourably to larger devices, the present one suggests high relevance of the regime also for future machines. More on the extrapolation will be provided in Section 4.

A type-II ELM definition exists at DIII-D by Snyder et al. [29], describing small type-I ELMs that are at the ballooning boundary. While the QCE pedestals in AUG are close to the ballooning limit, larger ELMs at lower separatrix density in the same plasma shape also exist here, as shown by Harrer et al. [16].

The enhanced D-alpha (EDA) mode from Alcator C-Mod [30,31] shares many features with the QCE regime, and the similarity to the type-II ELM regime was, in fact, already mentioned in the earliest publications, e.g. [8]. Small ELMs are observed in Alcator C-Mod in EDA when the normalised plasma pressure is above a certain threshold, $\beta_N > 1.3$ [31]. Below this threshold a *clean* EDA is observed, i.e. steady state without transients. The EDA H-mode is also observed in AUG [32,33] and DIII-D [34]. A quasi-coherent mode (QCM) serves as the identifier for the EDA H-mode. Similar mode structures are observed in type-II ELMs / QCE [8,23], with the spread of the mode frequency broadening in QCE compared to phases that can be unambiguously be identified as EDA phases (without visible filaments). In AUG during smooth transitions from EDA to QCE phases filaments develop only when the QCE is approached, and this transition is an active field of research, e.g. [23].

Another related type-I ELM-free regime comes with *grassy ELMs*. The expression originates from JT-60U [35]. Grassy ELMs are observed at high shaping together with high poloidal pressure β_{pol} , often reached at high safety factor and reduced plasma current. Along with JT-60U, the grassy ELM regime is reported from AUG [12], DIII-D [36] and EAST [37]. A main difference to the QCE regime is that in phases with grassy ELMs no quasi-coherent mode structure is reported [38,39]. The grassy ELMs are linked to high- n ballooning modes [40] similar to QCE, as shown in the following section.

3. Physics model

Dedicated studies in AUG revealed that the appearance of the QCE regime is related to processes near the separatrix [16], often called pedestal foot, a region in the range of poloidal flux label $\rho_{pol} \approx 0.99\text{--}0.999$ or about 1 mm inside the separatrix in absolute scale [22].

From the access conditions, i.e. strong shaping and high gas fuelling, a physics model is derived. Local ballooning modes are identified as candidates for the enhanced transport that leads to the flattening of the pressure gradient at the separatrix and a stabilisation of type-I ELMs. In the following, different ballooning modes are discussed.

3.1. Local ideal ballooning modes at the pedestal foot

Analysis of high confinement QCE plasmas with the ideal MHD stability code HELENA revealed that the pedestal foot is unstable to ideal, $n = \infty$ ballooning modes [18,19]. Further it was shown that QCE-relevant shapes destabilise the local ideal ballooning modes before the global peeling-balloonning limit of type-I ELMs is reached [26]. The relevant shaping parameter has the form [26]

$$S_d = \kappa^{2.2}(1 + \delta)^{0.9} \quad (1)$$

with elongation κ and averaged triangularity δ , which was identified to best represent the important physics. An operational window for QCE opens for $S_d > 3$. The mandatory minimum shaping parameter for a given experiment depends on the normalised pressure gradient both in the steep gradient region and at the pedestal foot and hence depends on fuelling, heating and safety factor. In addition, a potential link of the closeness to double-null on the ideal ballooning modes was shown in [18].

3.2. The turbulence parameter α_t

A related but somewhat different interpretation results from a drift-Alfvén turbulence model [41]. It was used to construct the separatrix operational space for different regimes in terms of density and temperature at the pedestal foot. A turbulence control parameter was defined [41]

$$\alpha_t = \frac{q_{cyl}}{100} v_{e,edge}^*. \quad (2)$$

The collisionality is

$$v_{e,edge}^* = 0.97 \times 10^{-16} \pi q_{cyl} \frac{n_{e,edge}}{T_{e,edge}^2} Z_{eff} \quad (3)$$

with major radius R_{geo} in (m), pedestal foot electron density $n_{e,edge}$ in (m^{-3}) and pedestal foot electron temperature $T_{e,edge}$ in (eV), further

$$q_{cyl} = \frac{B_{tor}}{B_{pol}} \frac{a_{geo}}{R_{geo}} \hat{\kappa} \quad (4)$$

$$B_{pol} = \frac{\mu_0 I_p}{2\pi a_{geo} \hat{\kappa}} \quad (5)$$

$$\hat{\kappa} = \sqrt{\frac{1 + \kappa^2(1 + 2\delta^2 - 1.2\delta^3)}{2}}. \quad (6)$$

Here, B_{tor} is the toroidal magnetic field on axis in (T), I_p the plasma current in (A), a_{geo} the minor radius in (m), μ_0 the vacuum permeability and Z_{eff} the effective charge at the pedestal foot.

The α_t parameter is linked to resistive ballooning mode stability [42]. Similarly to the ideal ballooning mode analysis, this model correlates $v_{e,edge}^*$ i.e. α_t to the suppression of type-I ELMs in AUG [22]. It was shown that for $\alpha_t > 0.55$ or $v_{e,edge}^* > 14$ type-I ELMs are avoided and the QCE regime is reached. In AUG reaching the ideal ballooning limit at the pedestal foot is only possible with simultaneously reaching $\alpha_t > 0.55$ [22]. Later, we will show that this is not necessarily true for future tokamaks.

Table 1

Main engineering parameters of AUG and JET in the QCE regime and design parameters of ITER and EU-DEMO.

	unit	AUG	JET	ITER	EU-DEMO
I_p	MA	0.6–1.0	1.5–2.25	15	18
B_{tor}	T	1.6–2.5	2.3–2.8	5.3	5.9
R_{geo}	m	1.6	2.9	6.2	9.1
a_{geo}	m	0.5	0.85	2.0	2.9
κ	–	1.5–1.88	1.75–1.88	1.85	1.86
δ	–	0.17–0.43	0.42–0.52	0.49	0.50
q_{cyl}	–	2.8–7.0	3.0–5.2	3.2	4.3
q_{95}	–	3.3–7.9	3.5–6.3	3.0	3.9
S_d	–	3.1–5.1	4.6–5.8	5.5	5.6

Studies at TCV showed a link between broadening of the scrape-off layer power fall-off length and α_t by both density and shaping variations [20,24]. In AUG the broadening of the scrape-off layer power fall-off length in QCE is linked to density or pressure at the pedestal foot and not α_t [22], while the limiter energy loads were found to increase with α_t in ELMY and QCE discharges [21]. The QCE regime is linked to the *density shoulder* [5,24,25], a flattening of the density gradient in the far-SOL which might enhance wall loads. The energy and particle load on limiters is an active field of research due to the potential of unwanted erosion and with this impurity influx in next step devices.

4. Comparison between ASDEX upgrade and JET and extrapolation to ITER and EU-DEMO

Now we turn to the comparison of the AUG and JET QCE operational spaces. The parameters from AUG are taken from a broad data set similar to the one published in [22], for JET we use the recent work presented in [27], including deuterium–tritium plasmas. Both tokamaks have metal plasma facing components.

4.1. Parameters

Global parameters for the four tokamaks are presented in [Table 1](#). The AUG and JET parameters do not represent the limits for achieving the QCE regime or the machine capabilities but present the achieved operational range within the utilised data sets. We will also present extrapolations for ITER and EU-DEMO. For ITER we take the design parameters of [43], for EU-DEMO we take the EU-DEMO-2018 design parameters of [44]. Further, we use the local parameters as presented in [Table 2](#) for the following calculations. The Greenwald density is defined as [45]

$$n_{\text{GW}} = 10^{14} \frac{I_p}{\pi a_{\text{geo}}^2} \quad (7)$$

with n_{GW} in (m^{-3}), I_p in (A) and a_{geo} in (m). We use the definition of [46] for the pedestal top collisionality

$$v_{\text{e,ped}}^* = 6.921 \times 10^{-18} \frac{Z_{\text{eff}} \ln A_e R_{\text{geo}} q_{95} n_{\text{e,ped}}}{(a_{\text{geo}}/R_{\text{geo}})^{1.5} T_{\text{e,ped}}^2} \quad (8)$$

with the Coulomb logarithm $\ln A_e$. For AUG and JET Z_{eff} results from line averaged measurements assuming flat profiles. The values for ITER and EU-DEMO have to be taken as indicative and do not necessarily represent official published estimates.

[Fig. 1](#) shows typical QCE experimental time traces for AUG and JET. Similar normalised global parameters are achieved in both tokamaks. With heating power levels needed to reach $\beta_N \approx 1.8–2.0$ both devices show a slightly reduced confinement scaling factor of $H_{98,y2} \approx 0.85–0.95$. The main parameters of AUG discharge # 39232 are $P_{\text{heat}} = 7.5 \text{ MW}$, $B_{\text{tor}} = 2.43 \text{ T}$, $I_p = 0.8 \text{ MA}$, $q_{\text{cyl}} = 4.9$. The main parameters of JET discharge JPN 105496 are $P_{\text{heat}} = 30 \text{ MW}$, $B_{\text{tor}} = 2.3 \text{ T}$, $I_p = 1.5 \text{ MA}$, $q_{\text{cyl}} = 3.9$.

Table 2

Main pedestal parameters of AUG, JET, ITER and EU-DEMO. The ITER and EU-DEMO values have to be taken as indicative and do not necessarily represent official estimates.

	unit	AUG	JET	ITER	EU-DEMO
n_{GW}	10^{19} m^{-3}	7–14	6–10	12.0	6.8
$n_{\text{e,ped}}$	10^{19} m^{-3}	3–12	3–8	8.0	5.7
$T_{\text{e,ped}}$	keV	0.2–0.5	0.7–1.0	4.7	3.7
$Z_{\text{eff,ped}}$	–	1.2–3.3	1.4–3.2	1.5	2.1
$Z_{\text{eff,edge}}$	–	N.A.	N.A.	2.0	2.5
P_{SOL}	MW	0.5–10	10–25	100	170
$v_{\text{e,ped}}^*$	–	1.6–25	0.9–2.0	0.06	0.21

The slightly reduced confinement scaling factor is in line with the observations in ELMY H-mode that an increased separatrix density reduces the pedestal top pressure [47]. The separatrix density is hence a crucial trade-off, it has to be high enough to reach QCE and fulfil the power exhaust requirements, but low enough to keep good confinement and additionally not reach an H-mode density limit [48–50].

The following subsections discuss the range of plasma shaping and the pedestal top values that are reached in AUG and JET QCE time windows together with the ITER and EU-DEMO design points. Further, an extrapolation of the pedestal foot parameters towards ITER and EU-DEMO for the necessary conditions to reach QCE using the two physics models described in [Section 3](#) is presented.

4.2. Plasma shaping

Strong plasma shaping is one of the key access conditions for QCE plasmas. [Fig. 2](#) presents a comparison of the shaping parameter S_d (Eq. (1)) and the safety factor q_{cyl} for the AUG and JET databases together with the expected values of ITER and EU-DEMO.

The AUG database is on average at higher q_{cyl} compared to the assumed values for ITER and EU-DEMO. The access to QCE was shown to be more difficult with lower safety factor, in line with both ideal and resistive MHD physics models. Nevertheless, the AUG database reaches values well within the designed EU-DEMO and ITER values. The JET database is on average at lower safety factor than AUG and close to the predictions for EU-DEMO and ITER.

The plasma shaping in AUG needed for QCE is less than in JET, while JET reaches shaping parameters very close to ITER and EU-DEMO. It is noteworthy that JET plasmas with reduced shaping did not show QCE phases [27], while the reduced (but still high) shaping is sufficient in AUG. A prediction of the necessary shaping for a given experiment needs the knowledge of the local pressure gradients. This is an important field of future studies, including potential size dependencies.

4.3. Pedestal top

[Fig. 3](#) compares two key pedestal top parameters, the collisionality and the Greenwald density fraction. While both AUG and JET reach the normalised pedestal densities expected for ITER and EU-DEMO, the reported values at TCV are lower. In all three tokamaks the collisionality is higher than the expected values in ITER and EU-DEMO. The spread in normalised density is mainly linked to the q_{cyl} variation in AUG and JET, and a higher Greenwald fraction relates to lower q_{cyl} . Due to the fact that the Greenwald density for ITER and EU-DEMO is within the probed space in AUG and JET, similar absolute densities are achieved as well. Since the pedestal pressure scales with tokamak size, lower pedestal top temperatures are achieved in the smaller plasmas. Hence, for the QCE regime in TCV, AUG and JET it is not possible to reach the same collisionality as expected for ITER and EU-DEMO. The lower collisionality in JET compared to AUG and TCV follows the expected trend with plasma size and reaches values as low as $v_{\text{e,ped}}^* = 0.9$, still an order of magnitude higher than expected in ITER.

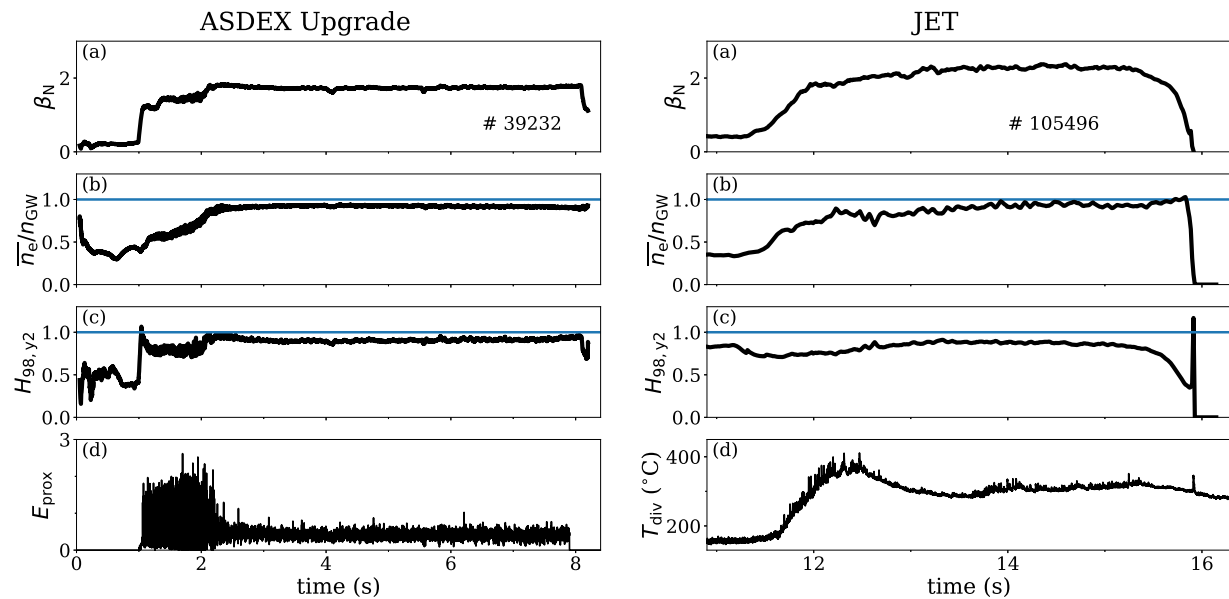


Fig. 1. Typical QCE plasmas in ASDEX Upgrade (left) and JET (right). (a) Normalised plasma pressure β_N , (b) normalised core density $n_{e,\text{core}}/n_{GW}$, (c) energy confinement factor H_{98,y^2} and (d) ELM monitor. The ELM monitor in ASDEX Upgrade is based on the outer divertor shunt current measurement (the definition is presented in [22]), for JET the outer divertor target temperature as measured by IR thermography is used. In both tokamaks, first a transient type-I ELM phase is present after the L-H transition. This is due to the shaping being increased only after the plasma pressure is on H-mode level, the QCE regime is then reached with the final shaping in both tokamaks and maintained for the full duration of the flat-top phase. The flat-top phase ends by a ramp-down of heating power starting at 8.1 s in AUG and 15.3 s in JET.

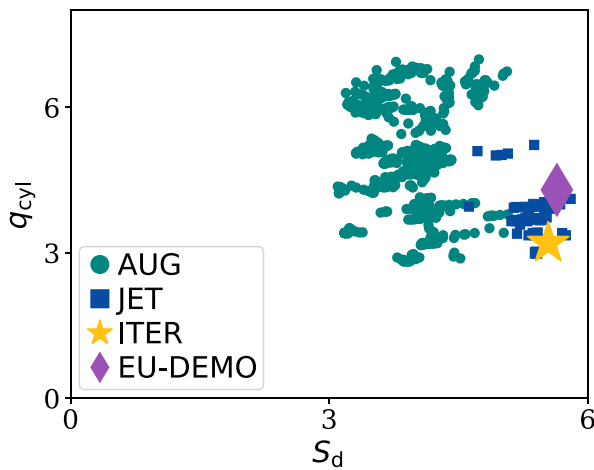


Fig. 2. Cylindrical safety factor q_{cyl} as a function of the shaping parameter S_d for the ASDEX Upgrade and JET data sets for time windows in QCE together with the design parameters for ITER and EU-DEMO. AUG typically operated at higher safety factor and lower shaping than ITER and EU-DEMO, reaching the design parameters of both machines within the data set. The JET data set is at comparable values for both safety factor and shaping with respect to ITER and EU-DEMO.

4.4. Pedestal foot

In the following, we calculate the local pedestal foot parameters for ITER and EU-DEMO that are needed to reach the QCE regime in accordance to the two physics models presented in Section 3, in the same way as presented in [22] with the assumption of Spitzer-Härm electron heat conduction being the dominant parallel loss channel in the scrape-off layer.

In the following, the data is interpreted in view of the two instabilities introduced above, the ideal ballooning mode α_{MHD} and the resistive ballooning mode as parameterised by α_l . An important open question not only for QCE is the amount of transport setting the gradients around the separatrix. Due to the lack of first-principle models for the transport across the separatrix (and near-SOL) the pressure gradient just

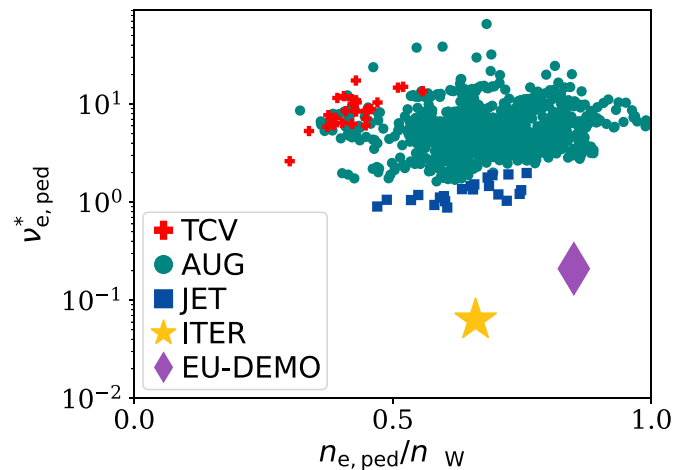


Fig. 3. Pedestal top collisionality as a function of the pedestal top density normalised to the Greenwald density for the TCV, ASDEX Upgrade and JET data sets for time windows in QCE together with the design parameters for ITER and EU-DEMO. The TCV data set is taken from [17]. Both AUG and JET reach the normalised density predicted for ITER and EU-DEMO but are at higher collisionality, while TCV is operated at lower normalised density. The lowest collisionality is reached in JET with $v_{e,\text{ped}}^* = 0.9$.

inside the separatrix and the power fall-off length in the near-SOL are unknown for ITER and EU-DEMO. Experimental work provides scaling laws that are typically used to extrapolate. In the following, we will rely on such scaling laws for the gradients or show the necessary gradients to fulfil the access conditions as proposed in Section 3.

While the majority of experiments are conducted in deuterium, JET offered the possibility to use also pure tritium and deuterium-tritium mixtures to gain insight into isotope effects. QCE experiments showed that results obtained in pure deuterium plasmas could be reproduced in mixed deuterium-tritium plasmas [27], while measurements of the inter-type-I ELM near-SOL power fall-off length did not show a change between deuterium and tritium plasmas [51].

Within this limitations, self-consistent extrapolations are shown.

4.4.1. Ideal ballooning mode

In this case we search for the minimum pedestal foot density for which $\alpha_{\text{MHD}} = \alpha_{\text{crit}}$ with

$$\alpha_{\text{MHD}} = 4\mu_0 R_{\text{geo}} q_{\text{cyl}}^2 n_{\text{e,edge}} T_{\text{e,edge}} \left\langle \lambda_{\text{p}_e} \right\rangle^{-1} \quad (9)$$

$$\alpha_{\text{crit}} = 0.64\kappa^{2.2}(1+\delta)^{0.9} = 0.64S_d, \quad (10)$$

with α_{crit} taken from [26]. For the pedestal foot pressure fall-off length we use a regression based on AUG QCE experiments [22]

$$\left\langle \lambda_{\text{p}_e} \right\rangle / \rho_{\text{s,pol}} = 1.30 \cdot (1 + 0.002 \cdot v_{\text{e,edge}}^{*2.0}), \quad (11)$$

with the poloidal gyro-radius

$$\rho_{\text{s,pol}} = \frac{\sqrt{m_i T_{\text{e,edge}}}}{e B_{\text{pol}}} \quad (12)$$

where m_i is the average ion mass. This represents a weak broadening due to collisionality. The brackets indicate that this is a poloidally averaged quantity. We assume further for the power fall-off length $\lambda_q = 21/10\lambda_{\text{p}_e}$ [52], i.e. no additional broadening in the near-SOL. The resulting parameter-sets are summarised in Table 3. For both ITER and EU-DEMO already at low density (normalised to Greenwald) of about $n_{\text{e,edge}}/n_{\text{GW}} \approx 0.25$ the critical pressure gradient is reached. It is speculated, that, if the local ballooning mode physics picture is correct, and the pressure gradient is steep (as predicted by the used scaling law and only modestly broader than the ITPA multi-machine regression for λ_q [53]) QCE should be achievable in both ITER and EU-DEMO at power exhaust relevant pedestal foot densities. We note that higher densities are not excluded, but they need to be accompanied by a broadening of the pressure gradient as explained in the next paragraph.

4.4.2. Resistive ballooning mode

In this case we search for a self-consistent set of gradients and local parameters to fulfil $\alpha_t = 0.55$. As it can be seen by the calculated α_t values for the α_{MHD} case, this is only possible with a broadening of the gradients. Here, we increase both λ_{p_e} and λ_q independently. We note that the power fall-off length was measured to significantly broaden in the QCE regime [5,20,22,24], deviating from the often observed link between pedestal foot pressure gradient and near-SOL power fall-off length [22]. The λ_{p_e} is assumed to broaden to stay below $\alpha_{\text{MHD}}/\alpha_{\text{crit}} = 1$, while λ_q is broadened to reach the desired α_t with the constraint of staying at $n_{\text{e,edge}}/n_{\text{GW}} = 0.5$. This is set as an arbitrary upper boundary for the density. With the broadening of λ_q the pedestal foot temperature reduces due to the Spitzer-Härm electron heat conduction assumption [22] and with this increases α_t until reaching the desired value. The resulting parameter-sets are summarised in Table 3. For both ITER and EU-DEMO reaching $\alpha_t = 0.55$ is more restrictive than $\alpha_{\text{MHD}}/\alpha_{\text{crit}} = 1$. A significant broadening of λ_q needs to be assumed. It has to be noted that the calculated λ_q values are still lower than the XGC1 code predictions for ITER [54]. Using a critical $v_{\text{e,edge}}^*$ instead of α_t leads to very similar extrapolations as shown in [22].

4.4.3. Implications

For AUG and JET, reaching the ideal ballooning limit is simultaneously reaching $\alpha_t > 0.55$ [22,26], this is no longer necessarily true for ITER and EU-DEMO. While there is room to reduce $T_{\text{e,edge}}$ in AUG and JET experiments by reducing the heating power, therefore reducing α_{MHD} and increasing α_t , this might not be possible for ITER and EU-DEMO due to the constraint of staying above the H-mode threshold power. It is therefore important to study the access to QCE in detail and to distinguish the two access conditions in order to be able to extrapolate with more confidence to new machines. We also point out that so far only the onset threshold for the pedestal foot ballooning modes has been treated and no non-linear or quasi-linear model for the transport driven by these modes exists. It is, hence, not yet possible to extrapolate if the transport levels are sufficient in order to keep the pedestal from reaching the global peeling-balloon mode limit.

Table 3

Local plasma parameters required at the pedestal foot of the plasma, 1 mm inside of the separatrix of ITER and EU-DEMO for reaching QCE given the physics models based on ideal ballooning modes (α_{MHD}) or on the $\alpha_t \geq 0.55$ criterion.

unit	ITER - α_{MHD}	ITER - α_t	EU-DEMO - α_{MHD}	EU-DEMO - α_t
$\langle \lambda_{\text{p}_e} \rangle$ mm	4.0	5.3	5.3	6.5
λ_q mm	1.1	3.4	1.4	4.2
$n_{\text{e,edge}}$ 10^{19} m^{-3}	3.0	5.7	1.6	2.7
$T_{\text{e,edge}}$ eV	264	183	329	225
α_t	-	0.14	0.55	0.16

5. Summary and outlook

The QCE regime has been extensively studied in recent years in both AUG and JET. The regime is accessed at high plasma shaping and sufficient fuelling with ideal or resistive ballooning modes close to the separatrix being candidates to explain the type-I ELM stabilisation. The QCE regime in JET was achieved by following techniques developed in AUG and TCV.

Using AUG and JET as a step-ladder, a first extrapolation towards ITER and EU-DEMO parameters is presented. The shaping and safety factor of ITER and EU-DEMO is within the parameters in JET and AUG. Due to the fact that QCE is a high density regime, the pedestal top density values are well within the expected range in ITER and EU-DEMO. The pedestal top collisionality is higher, though recent experiments are getting closer to the value expected in ITER and EU-DEMO, as the JET experiments achieved values as low as $v_{\text{e,ped}}^* = 0.9$ [27].

Based on the described physics models, an extrapolation is carried out for ITER and EU-DEMO for the access to the QCE regime. The necessary pedestal foot density to reach the ideal ballooning limit for both tokamaks is about $n_{\text{e,edge}}/n_{\text{GW}} \approx 0.25$ assuming the applied pressure gradient scaling is justified. This is well within the typically achievable pedestal foot density range. On the other hand, reaching the criterion $\alpha_t > 0.55$ is more challenging. Realistic densities, here using $n_{\text{e,edge}}/n_{\text{GW}} = 0.5$, are compatible with this criterion only when assuming a broadening of the power fall-off length. Such a broadening is indeed observed in QCE discharges in AUG [5,22] and TCV [20,24].

Two key open questions still need to be addressed in future work. First, the quantification of the transport associated to the local MHD modes is missing, e.g. at present we can only scale the access criteria as a first step. Second, no scaling of the filament impact on the divertor and first wall exists so far. Especially a potential buffering of the filaments before reaching the divertor target is an important field of future studies. So far partial detachment is reported in between filaments, while the filaments are attached [22]. We conclude that the QCE regime is a promising reactor-scenario due to the absence of ELMs, the potential broadening of the power fall-off length and the compatibility with high pedestal foot density.

CRediT authorship contribution statement

M. Faitsch: Writing – review & editing, Writing – original draft, Investigation, Formal analysis, Conceptualization. **M. Dunne:** Writing – review & editing, Investigation, Formal analysis, Conceptualization. **E. Lerche:** Writing – review & editing, Investigation, Formal analysis. **P. Lomas:** Investigation. **I. Balboa:** Formal analysis. **P. Bilkova:** Formal analysis. **P. Bohm:** Formal analysis. **L. Gil:** Writing – review & editing, Investigation. **G.F. Harrer:** Investigation. **A. Kappatou:** Writing – review & editing, Project administration. **D. Kos:** Formal analysis. **B. Labit:** Project administration. **L. Radovanovic:** Writing – review & editing, Investigation. **A. Redl:** Investigation. **O. Sauter:** Investigation. **S. Silburn:** Formal analysis. **E.R. Solano:** Investigation. **A. Tookey:** Formal analysis. **E. Viezzer:** Investigation. **E. Wolfrum:** Writing – review & editing, Investigation. **U. Stroth:** Writing – review & editing, Supervision, Funding acquisition.

Declaration of competing interest

The authors declare the following financial interests/personal relationships which may be considered as potential competing interests: M. Faitsch reports financial support was provided by Euratom Research and Training Programme. B. Labit, O. Sauter reports financial support was provided by Swiss State Secretariat for Education Research and Innovation. E.R. Solano reports financial support was provided by European Regional Development Fund. If there are other authors, they declare that they have no known competing financial interests or personal relationships that could have appeared to influence the work reported in this paper.

Acknowledgements

This work has been carried out within the framework of the EU-ROfusion Consortium, partially funded by the European Union via the Euratom Research and Training Programme (Grant Agreement No 101052200 — EUROfusion). The Swiss contribution to this work has been funded by the Swiss State Secretariat for Education, Research and Innovation (SERI). Views and opinions expressed are however those of the author(s) only and do not necessarily reflect those of the European Union, the European Commission or SERI. Neither the European Union nor the European Commission nor SERI can be held responsible for them. Work supported in part by a grant PID2021-127727OB-I00 funded by the Spanish MCIN/AEI/10.13039/501100011033 and by ERDF “A way of making Europe”.

Data availability

Data will be made available on request.

References

- [1] H. Zohm, Edge localized modes (ELMs), *Plasma Phys. Control. Fusion* 38 (2) (1996) 105.
- [2] ITER Physics Basis Editors, ITER Physics Expert Group Chairs and Co-Chairs, *ITER Joint Central Team and Physics Integration Unit, Chapter 1: Overview and summary*, *Nucl. Fusion* 39 (12) (1999) 2137.
- [3] A. Loarte, G. Huijsmans, S. Futatani, L. Baylor, T. Evans, D.M. Orlov, O. Schmitz, M. Becoulet, P. Cahyna, Y. Gribov, A. Kavin, A.S. Naik, D. Campbell, T. Casper, E. Daly, H. Frerichs, A. Kischner, R. Laengner, S. Lisgo, R. Pitts, G. Saibene, A. Wingen, Progress on the application of ELM control schemes to ITER scenarios from the non-active phase to DT operation, *Nucl. Fusion* 54 (3) (2014) 033007.
- [4] T. Eich, B. Sieglin, A. Thornton, M. Faitsch, A. Kirk, A. Herrmann, W. Suttrop, ELM divertor peak energy fluence scaling to ITER with data from JET, MAST, and ASDEX Upgrade, *Nucl. Mater. Energy* 12 (Suppl. C) (2017) 84–90.
- [5] M. Faitsch, T. Eich, G. Harrer, E. Wolfrum, D. Brida, P. David, M. Griener, U. Stroth, Broadening of the power fall-off length in a high density, high confinement H-mode regime in ASDEX Upgrade, *Nucl. Mater. Energy* 26 (2021) 100890.
- [6] E. Viezzier, M. Austin, M. Bernert, K. Burrell, P. Cano-Megias, X. Chen, D. Cruz-Zabala, S. Coda, M. Faitsch, O. Février, L. Gil, C. Giroud, T. Happel, G. Harrer, A. Hubbard, J. Hughes, A. Kallenbach, B. Labit, A. Merle, H. Meyer, C. Paz-Soldan, P. Oyola, O. Sauter, M. Siccino, D. Silvagni, E. Solano, Prospects of core-edge integrated no-ELM and small-ELM scenarios for future fusion devices, *Nucl. Mater. Energy* 34 (2023) 101308.
- [7] U. Stroth, D. Aguiam, E. Alessi, C. Angioni, N. Arden, R.A. Parra, V. Artigues, O. Asunta, M. Balden, V. Bandaru, A. Banon-Navarro, K. Behler, A. Bergmann, M. Bergmann, J. Bernardo, M. Bernert, A. Biancalani, R. Bielajew, R. Bilato, G. Birkenmeier, T. Blanken, V. Bobkov, A. Bock, T. Body, T. Bolzonella, N. Bonanomi, A. Bortolon, B. Böswirth, C. Bottereau, A. Bottino, H. van den Brand, M. Brenzke, S. Brezinsek, D. Brida, F. Brochard, C. Bruhn, J. Buchanan, A. Buhler, A. Burckhart, Y. Camenen, B. Cannas, P.C. Megias, D. Carlton, M. Carr, P. Carvalho, C. Castaldo, M. Cavedon, C. Cazzaniga, C. Challis, A. Chankin, C. Cianfarani, F. Clairet, S. Coda, R. Coelho, J. Coenen, L. Colas, G. Conway, S. Costea, D. Coster, T. Cote, A. Creely, G. Croci, D.C. Zabala, G. Cseh, A. Czarnecka, I. Cziegler, O. D’Arcangelo, A.D. Molin, P. David, C. Day, M. de Baar, P. de Marné, R. Delogu, S. Denk, P. Denner, A. Di Siena, J.D.P. Durán, D. Dunai, A. Drenik, M. Dreval, R. Drube, M. Dunne, B. Duval, R. Dux, T. Eich, S. Elgeti, A. Encheva, K. Engelhardt, B. Erdös, I. Erofeev, B. Esposito, E. Fable, M. Faitsch, U. Fantz, M. Farnik, H. Faugel, F. Felici, O. Ficker, S. Fietz, A. Figueiredo, R. Fischer, O. Ford, L. Frassinetti, M. Fröschele, G. Fuchert, J. Fuchs, H. Fünfgelder, S. Futatani, K. Galazka, J. Galdon-Quiroga, D.G. Escolà, A. Gallo, Y. Gao, S. Garavaglia, M.G. Muñoz, B. Geiger, L. Giannone, S. Gibson, L. Gil, E. Giovannozzi, S. Glöggler, M. Gobbin, J.G. Martin, T. Goodman, G. Gorini, T. Görler, D. Gradic, G. Granucci, A. Gräter, H. Greuner, M. Griener, M. Groth, A. Gude, L. Guimaraes, S. Günter, G. Haas, A. Hakola, C. Ham, T. Happel, N. den Harder, G. Harrer, J. Harrison, V. Hauer, T. Hayward-Schneider, B. Heinemann, T. Hellsten, S. Henderson, P. Hennequin, A. Herrmann, E. Heyn, F. Hitzler, J. Hobirk, K. Höfler, J. Holm, M. Hözl, C. Hopf, L. Horvath, T. Höschens, A. Houben, A. Hubbard, A. Huber, K. Hunger, V. Igochine, M. Iliasova, T. Ilkei, K.I. Björk, C. Ionita-Schriftwieser, I. Ivanova-Stanik, W. Jacob, N. Jaksic, F. Janký, A.J. van Vuuren, A. Jardin, F. Jaulmes, F. Jenko, T. Jensen, E. Joffrin, A. Kallenbach, S. Kálvin, M. Kantor, A. Kappatou, O. Kardaun, J. Karhunen, C.-P. Käsemann, S. Kasilov, A. Kendl, W. Kernbichler, E. Khilkevitch, A. Kirk, S.K. Hansen, V. Klevarova, G. Kocsis, M. Koleva, M. Komm, M. Kong, A. Krämer-Flecken, K. Krieger, A. Krivska, O. Kudlacek, T. Kurki-Suonio, B. Kurzan, B. Labit, K. Lackner, F. Laggner, A. Lahtinen, P. Lang, P. Lauber, N. Leuthold, L. Li, J. Likonen, O. Linder, B. Lipschultz, Y. Liu, A. Lohs, Z. Lu, T.L. di Cortemiglia, N. Luhmann, T. Lunt, A. Lyssoivan, T. Maceina, J. Madsen, A. Magnanimo, H. Maier, J. Mailoux, R. Maingi, O. Maj, E. Maljaars, P. Manas, A. Mancini, A. Manhard, P. Mantica, M. Mansinsen, P. Manz, M. Maraschek, C. Marchetto, L. Marrelli, P. Martin, A. Martitsch, F. Matos, M. Mayer, M.-L. Mayoral, D. Mazon, P. McCarthy, R. McDermott, R. Merkel, A. Merle, D. Meshcheriakov, H. Meyer, D. Milanesio, P.M. Cabrera, F. Monaco, M. Muraca, F. Nabais, V. Naulin, R. Nazikian, R. Nem, A. Nemes-Czopf, G. Neu, R. Neu, A. Nielsen, S. Nielsen, T. Nishizawa, M. Nocente, J.-M. Noterdaeme, I. Novikau, S. Nowak, M. Oberkofer, R. Ochoukov, J. Olsen, F. Orain, F. Palermo, O. Pan, G. Papp, I.P. Perez, A. Pau, G. Pautasso, C. Paz-Soldan, P. Petersson, P. Piovesan, C. Piron, U. Plank, B. Plaum, B. Plöck, V. Plyusnin, G. Pokol, E. Poli, L. Porte, T. Pütterich, M. Ramisch, J. Rasmussen, G. Ratta, S. Ratynskaia, G. Raupp, D. Réfy, M. Reich, F. Reimold, D. Reiser, M. Reisner, D. Reiter, T. Ribeiro, R. Riedl, J. Riesch, D. Rittich, J.R. Rodriguez, G. Rocchi, P. Rodriguez-Fernandez, M. Rodriguez-Ramos, V. Rohde, G. Ronchi, A. Ross, M. Rott, M. Rubel, D. Ryan, F. Ryter, S. Saarelma, M. Salewski, A. Salmi, O. Samoylov, L.S. Sanchez, J. Santos, O. Sauter, G. Schall, K. Schlüter, K. Schmid, O. Schmitz, P. Schneider, R. Schriftwieser, M. Schubert, C. Schuster, T. Schwarz-Selingher, J. Schweinzer, E. Seluin, A. Shabbir, A. Shalpegin, S. Sharapov, U. Sheikh, A. Shevelev, G. Sias, M. Siccino, B. Sieglin, A. Sigalov, A. Silva, C. Silva, D. Silvagni, J. Simpson, S. Sipilä, E. Smigelskis, A. Snicker, E. Solano, C. Sommariva, C. Sozzi, G. Spizzo, M. Spolaore, A. Stegmeir, M. Stejner, J. Stober, E. Strumberge, G.S. Lopez, H.-J. Sun, W. Suttrop, E. Sytova, T. Szepesi, B. Tál, T. Tala, G. Tardini, M. Tardocchi, D. Terranova, M. Teschke, E. Thorén, W. Tierens, D. Told, W. Treutterer, G. Trevisan, E. Trier, M. Tripský, M. Usoltceva, M. Valisa, M. Valovic, M. van Zeeland, F. Vannini, B. Vanovac, P. Varela, S. Varoutis, N. Vianello, J. Vicente, G. Verdooleage, T. Vierle, E. Viezzier, I. Voitsekhovitch, U. von Toussaint, D. Wagner, X. Wang, M. Weiland, A. White, M. Willensdorfer, B. Wiringer, M. Wischmeier, R. Wolf, E. Wolfrum, Q. Yang, Q. Yu, R. Zagórski, I. Zammuto, T. Zehetbauer, W. Zhang, W. Zhlobenko, M. Zilker, A. Zito, H. Zohm, S. Zolezník, the EUROfusion MST1 Team, Progress from ASDEX upgrade experiments in preparing the physics basis of ITER operation and DEMO scenario development, *Nucl. Fusion* 62 (4) (2022) 042006.
- [8] J. Stober, M. Maraschek, G. Conway, O. Gruber, A. Herrmann, A. Sips, W. Treutterer, H. Zohm, ASDEX Upgrade Team, Type II ELMy H modes on ASDEX upgrade with good confinement at high density, *Nucl. Fusion* 41 (9) (2001) 1123–1134.
- [9] C. Perez von Thun, M. Maraschek, S. da Graça, R.J. Buttery, A. Herrmann, J. Stober, G. Conway, T. Eich, J.C. Fuchs, L.D. Horton, V. Igochine, A. Kallenbach, A. Loarte, H.W. Müller, I. Nunes, G. Saibene, R. Sartori, A.C.C. Sips, W. Suttrop, E. Wolfrum, the ASDEX Upgrade Team, Identifying the MHD signature and power deposition characteristics associated with type-II ELMs in ASDEX upgrade, *Plasma Phys. Control. Fusion* 50 (6) (2008) 065018.
- [10] E. Wolfrum, M. Bernert, J.E. Boom, A. Burckhart, I.G.J. Classen, G.D. Conway, T. Eich, R. Fischer, A. Gude, A. Herrmann, N.C. Luhmann, M. Maraschek, R. McDermott, H.K. Park, T. Pütterich, J. Vicente, B. Wieland, M. Willensdorfer, the ASDEX Upgrade Team, Characterization of edge profiles and fluctuations in discharges with type-II and nitrogen-mitigated edge localized modes in ASDEX upgrade, *Plasma Phys. Control. Fusion* 53 (8) (2011) 085026.
- [11] G. Saibene, P. Lomas, R. Sartori, A. Loarte, J. Stober, Y. Andrew, S. Arshad, G. Conway, E. de la Luna, K. Günther, L. Ingesson, M. Kempenaars, A. Korotkov, H. Koslowski, J. Lönnroth, D. McDonald, A. Meigs, P. Monier-Garbet, V. Parail, C. Perez, F. Rimini, S. Sharapov, P. Thomas, Characterization of small ELM experiments in highly shaped single null and quasi-double-null plasmas in JET, *Nucl. Fusion* 45 (5) (2005) 297–317.
- [12] J. Stober, P. Lomas, G. Saibene, Y. Andrew, P. Belo, G. Conway, A. Herrmann, L. Horton, M. Kempenaars, H.-R. Koslowski, A. Loarte, G. Maddison, M. Maraschek, D. McDonald, A. Meigs, P. Monier-Garbet, D. Mossessian, M. Nave, N. Oyama, V. Parail, C. Perez, F. Rimini, R. Sartori, A. Sips, P. Thomas, Contributors to the EFDA-JET workprogramme, the ASDEX Upgrade Team, Small ELM regimes with good confinement on JET and comparison to those on ASDEX Upgrade, alcator C-mod and JT-60U, *Nucl. Fusion* 45 (11) (2005) 1213.

- [13] C. Perez von Thun, R. Buttery, A. Loarte, P. Lomas, G. Maddison, M. Maraschek, I. Nunes, G. Saibene, R. Sartori, J. Stober, JET EFDA contributors, On the properties of edge localised density fluctuations observed in quasi-double null identity experiments in JET, in: Proceedings of the 34th EPS Conference on Plasma Physics, 2007.
- [14] I. Nunes, G. Saibene, R. Sartori, P. Lomas, C. Perez, S. Saarelma, A. Alfier, Y. Andrew, G. Arnoux, M. Beurskens, A. Boboc, I. Coffey, K. Crombe, E. Giovannozzi, M. Kempenaars, K. Lawson, H. Leggate, E. de la Luna, C. McKenna, V. Parail, R. Pasqualotto, the JET EFDA contributors, Small ELMs in quasi-double null plasmas at JET, in: Proceedings of the 34th EPS Conference on Plasma Physics, 2007.
- [15] A. Kirk, H.W. Muller, E. Wolfrum, H. Meyer, A. Herrmann, T. Lunt, V. Rohde, P. Tamain, the MAST and ASDEX Upgrade Team, Comparison of small edge-localized modes on MAST and ASDEX upgrade, *Plasma Phys. Control. Fusion* 53 (9) (2011) 095008.
- [16] G. Harrer, E. Wolfrum, M. Dunne, P. Manz, M. Cavedon, P. Lang, B. Kurzan, T. Eich, B. Labit, J. Stober, H. Meyer, M. Bernert, F. Laggner, F. Aumayr, the EUROfusion MST1 Team, the ASDEX Upgrade Team, Parameter dependences of small edge localized modes (ELMs), *Nucl. Fusion* 58 (11) (2018) 112001.
- [17] B. Labit, T. Eich, G. Harrer, E. Wolfrum, M. Bernert, M. Dunne, L. Frassinetti, P. Hennquin, R. Maurizio, A. Merle, H. Meyer, S. Saarelma, U. Sheikh, J. Adamek, M. Agostini, D. Aguiam, R. Akers, R. Albanese, C. Albert, E. Alessi, R. Ambrosino, Y. André, C. Angioni, G. Apruzzese, M. Aradi, H. Arnichand, F. Auriemma, G. Avdeeva, J. Aylón-Guerola, F. Bagnato, V. Bandaru, M. Barnes, L. Barrera-Orte, P. Bettini, R. Bilato, O. Biletskyi, P. Bilkova, W. Bin, P. Blanchard, T. Blanken, V. Bobkov, A. Bock, D. Boeyaert, K. Bogar, O. Bogar, P. Bohm, T. Bolzonella, F. Bombarda, L. Boncagni, F. Bouquey, C. Bowman, S. Brezinsek, D. Brida, D. Brunetti, J. Bucalossi, J. Buchanan, J. Buermans, H. Bufferand, S. Buller, P. Buratti, A. Burckhart, G. Calabro, L. Calacchi, Y. Camenen, B. Cannas, P.C. Megías, D. Carnevale, F. Carpanese, M. Carr, D. Carralero, L. Carraro, A. Casolari, A. Cathey, F. Causa, M. Cavedon, M. Ceccarello, S. Ceccuzzi, J. Cerovsky, S. Chapman, P. Chmielewski, D. Choi, C. Cianfarani, G. Ciraolo, S. Coda, R. Coelho, L. Colas, D. Colette, L. Cordaro, F. Cordella, S. Costea, D. Coster, D.C. Zubala, G. Cseh, A. Czarnecka, I. Czegler, O. D'Arcangelo, A.D. Molin, P. David, G.D. Carolis, H.D. Oliveira, J. Decker, R. Dejarnac, R. Delogu, N. den Harder, M. Dimitrova, F. Dolizy, J.D.-P. Durán, D. Douai, A. Drenik, M. Dreval, B. Dudson, D. Dunai, B. Duval, R. Dux, S. Elmore, O. Embreus, B. Erdős, E. Fable, M. Faitsch, A. Fanni, M. Farnik, I. Faust, J. Faustin, N. Fedorczak, F. Felici, S. Feng, X. Feng, J. Ferreira, G. Ferrò, O. Février, O. Ficker, L. Figini, A. Figueiredo, A. Fil, M. Fontana, M. Francesco, C. Fuchs, S. Futatani, L. Gabellieri, D. Gadariya, D. Gahle, D. Galassi, K. Galazka, J. Galdon-Quiroga, S. Galeani, D. Gallart, A. Gallo, C. Galperti, S. Garavaglia, J. Garcia, J. Garcia-Lopez, M. Garcia-Muñoz, L. Garzotti, J. Gath, B. Geiger, L. Giacomelli, L. Giannone, S. Gibson, L. Gil, E. Giovannozzi, G. Giruzzi, M. Gobbin, J. Gonzalez-Martin, T. Goodman, G. Gorini, M. Gospodarczyk, G. Granucci, D. Grekov, G. Grenfell, M. Griener, M. Groth, O. Grover, M. Grueca, A. Gude, L. Guimaraes, T. Gyergyek, P. Hacek, A. Hakola, C. Ham, T. Happel, J. Harrison, A. Havranek, J. Hawke, S. Henderson, L. Hesslow, F. Hitzler, B. Hnat, J. Hobirk, M. Högl, D. Hogeweij, C. Hopf, M. Hoppe, J. Horacek, M. Hron, Z. Huang, A. Iantchenko, D. Iglesias, V. Igochine, P. Innocente, C. Ionita-Schriftwieser, H. Isliker, I. Ivanova-Stanik, A. Jacobsen, M. Jakubowski, F. Janký, A. Jardin, F. Jaulmes, T. Jensen, T. Jonsson, A. Kallenbach, A. Kappatou, A. Karpushov, S. Kasilov, Y. Kazakov, P. Kazantzidis, D. Keeling, M. Kelemen, A. Kendl, W. Kernbichler, A. Kirk, G. Kocsis, M. Komm, M. Kong, V. Korovin, M. Koubití, J. Kovacic, N. Krawczyk, K. Krieger, L. Kripner, A. Křivská, O. Kudlacek, Y. Kulyk, T. Kurki-Suonio, R. Kwiatkowski, F. Laggner, L. Laguardia, A. Lahtinen, P. Lang, J. Likonen, B. Lipschultz, F. Liu, R. Lombroni, R. Lorenzini, V. Loschiavo, T. Lunt, E. Macusova, J. Madsen, R. Maggiore, B. Maljaars, P. Manas, P. Mantica, M. Mantsinen, P. Manz, M. Maraschek, V. Marchenko, C. Marchetto, A. Mariani, C. Marini, T. Markovic, L. Marrelli, P. Martin, J.M. Solis, A. Martitsch, S. Mastrostefano, F. Matos, G. Matthews, M.-L. Mayoral, D. Mazon, C. Mazzotta, P.M. Carthy, K. McClements, R. McDermott, B. Mcmillan, C. Meineri, V. Menkovski, D. Meshcheriakov, M. Messmer, D. Micheletti, D. Milanesio, F. Milletello, I. Miron, J. Mlynar, V. Moiseenko, P.M. Cabrera, J. Morales, J.-M. Moret, A. Moro, D. Moulton, F. Nabais, V. Naulin, D. Naydenkova, R. Nem, F. Nespoli, S. Newton, A. Nielsen, S. Nielsen, V. Nikolaeva, M. Nocente, S. Nowak, M. Oberkofler, R. Ochoukov, P. Ollus, J. Olsen, J. Omotani, J. Ongeña, F. Orain, F. Orsitti, R. Paccagnella, A. Palha, L. Panaccione, R. Panek, M. Panjan, G. Papp, I.P. Perez, F. Parra, M. Passeri, A. Pau, G. Pautasso, R. Pavlichenko, A. Perek, V.P. Radolfini, F. Pesamosca, M. Peterka, V. Petrzilka, V. Piergotti, L. Pigatto, P. Piovesan, C. Piron, L. Piron, V. Plyusnin, G. Pokol, E. Poli, P. Pölöskei, T. Popov, Z. Popovic, G. Pór, L. Porte, G. Puccella, M. Puiatti, T. Pütterich, M. Rabinski, J.J. Rasmussen, J. Rasmussen, G. Rattá, S. Ratynskaia, T. Ravensbergen, D. Réfy, M. Reich, H. Reimerdes, F. Reimold, D. Reiser, C. Reux, S. Reznik, D. Ricci, N. Rispoli, J. Rivero-Rodriguez, G. Rocchi, M. Rodriguez-Ramos, A. Romano, J. Rosato, G. Rubinacci, G. Rubino, D. Ryan, M. Salewski, A. Salmi, D. Samaddar, L. Sanchis-Sánchez, J. Santos, K. Särkimäki, M. Sassano, O. Sauter, R. Scannell, M. Scheffer, B. Schneider, P. Schneider, R. Schriftwieser, M. Schubert, J. Seidl, E. Seliunin, S. Sharapov, R. Sheeba, G. Sias, B. Sieglin, C. Silva, S. Sipilä, S. Smith, A. Snicker, E. Solano, S. Hansen, C. Soria-Hoyo, E. Sorokovoy, C. Sozzi, A. Sperduto, G. Spizzo, M. Spolaoore, M. Stejner, L. Stipani, J. Stober, P. Strand, H. Sun, W. Sutrop, D. Sytnykov, T. Szepesi, B. Tál, T. Tala, G. Tardini, M. Tardocchi, A. Teplukhina, D. Terranova, D. Testa, C. Theiler, E. Thorén, A. Thornton, B. Tilia, P. Tolias, M. Tomes, M. Toscano-Jimenez, C. Tsironis, C. Tsui, O. Tudisco, J. Urban, M. Valisa, M. Vallar, P.V. Olivares, M. Valovic, D.V. Vugt, B. Vanovac, J. Varju, S. Varoutis, S. Vartanian, O. Vasilevici, J. Vega, G. Verdoolege, K. Verhaegh, L. Vermare, N. Vianello, J. Vicente, E. Viezzier, F. Villone, I. Voitsekhovich, D. Voltolina, P. Vondracek, N. Vu, N. Walkden, T. Wauters, M. Weiland, V. Weinzel, M. Wensing, S. Wiesen, M. Wiesenberger, G. Wilkie, M. Willensdorfer, M. Wischmeier, K. Wu, L. Xiang, R. Zagorski, D. Zaloga, P. Zanca, R. Zaplotnik, J. Zebrowski, W. Zhang, A. Zisis, S. Zoletnik, M. Zuin, Dependence on plasma shape and plasma fueling for small edge-localized mode regimes in TCV and ASDEX upgrade, *Nucl. Fusion* 59 (8) (2019) 086020.
- [18] G.F. Harrer, M. Faitsch, L. Radovanovic, E. Wolfrum, C. Albert, A. Cathey, M. Cavedon, M. Dunne, T. Eich, R. Fischer, M. Griener, M. Hoelzl, B. Labit, H. Meyer, F. Aumayr, The ASDEX Upgrade Team, The EUROfusion MST1 Team, Quasicontinuous exhaust scenario for a fusion reactor: The renaissance of small edge localized modes, *Phys. Rev. Lett.* 129 (2022) 165001.
- [19] L. Radovanovic, M. Dunne, E. Wolfrum, G. Harrer, M. Faitsch, R. Fischer, F. Aumayr, Developing a physics understanding of the quasi-continuous exhaust regime: pedestal profile and ballooning stability analysis, *Nucl. Fusion* 62 (8) (2022) 086004.
- [20] A. Stagni, N. Vianello, C. Tsui, C. Colandrea, S. Gorno, M. Bernert, J. Boedo, D. Brida, G. Falchetto, A. Hakola, G. Harrer, H. Reimerdes, C. Theiler, E. Tsitrone, N. Walkden, the TCV Team, the EUROfusion MST1 Team, Dependence of scrape-off layer profiles and turbulence on gas fuelling in high density H-mode regimes in TCV, *Nucl. Fusion* 62 (9) (2022) 096031.
- [21] A. Redl, T. Eich, N. Vianello, P. David, Energy load on first wall components in high density, small ELM regimes in ASDEX upgrade, *Nucl. Mater. Energy* 34 (2023) 101319.
- [22] M. Faitsch, T. Eich, G. Harrer, E. Wolfrum, D. Brida, P. David, M. Dunne, L. Gil, B. Labit, U. Stroth, the ASDEX Upgrade Team, the EUROfusion MST1 Team, Analysis and expansion of the quasi-continuous exhaust (QCE) regime in ASDEX upgrade, *Nucl. Fusion* 63 (7) (2023) 076013.
- [23] J. Kalis, G. Birkenmeier, P. Manz, T. Eich, M. Griener, R. Goti, M. Cavedon, L. Gil, M. Faitsch, L. Radovanovic, D. Wendler, E. Wolfrum, U. Stroth, the ASDEX Upgrade Team, the EUROfusion MST1 Team, Experimental characterization of the quasi-coherent mode in EDA H-Mode and QCE scenarios at ASDEX Upgrade, *Nucl. Fusion* 64 (1) (2023) 016038.
- [24] A. Stagni, N. Vianello, M. Agostini, C. Colandrea, S. Gorno, B. Labit, U. Sheikh, L. Simons, G. Sun, C. Tsui, M. Ugoletti, Y. Wang, C. Wüthrich, J. Boedo, H. Reimerdes, C. Theiler, the TCV Team, The effect of plasma shaping on high density H-mode SOL profiles and fluctuations in TCV, *Nucl. Fusion* 64 (2) (2024) 026016.
- [25] A. Redl, T. Eich, N. Vianello, P. David, J. Adamek, M. Bernert, G. Birkenmeier, D. Brida, P. David, M. Faitsch, R. Fischer, G. Grenfell, R. Ochoukov, V. Rohde, B. Tal, M. Dreval, An extensive analysis of SOL properties in high-delta plasmas in asdex upgrade, *Nucl. Fusion* (2024).
- [26] M. Dunne, M. Faitsch, L. Radovanovic, E. Wolfrum, the ASDEX Upgrade Team, Quasi-continuous exhaust operational space, *Nucl. Fusion* 64 (12) (2024) 124003.
- [27] M. Faitsch, M. Dunne, E. Lerche, P. Lomas, I. Balboa, P. Bilkova, P. Bohm, A. Kappatou, D. Kos, B. Labit, S. Menmuir, O. Sauter, S. Silburn, E. Solano, H. Sun, A. Tookey, E. Viezzier, U. Stroth, JET Contributors, the EUROfusion Tokamak Exploitation Team, The quasi-continuous exhaust regime in JET, *Nucl. Fusion* 65 (2) (2025) 024003.
- [28] S. Saarelma, S. Günter, L. Horton, t.A.U. Team, MHD stability analysis of type II ELMs in ASDEX Upgrade, *Nucl. Fusion* 43 (4) (2003) 262–267.
- [29] P. Snyder, H. Wilson, J. Ferron, L. Lao, A. Leonard, D. Mossessian, M. Murakami, T. Osborne, A. Turnbull, X. Xu, ELMs and constraints on the H-mode pedestal: peeling-ballooning stability calculation and comparison with experiment, *Nucl. Fusion* 44 (2) (2004) 320.
- [30] Y. Takase, R. Boivin, F. Bombarda, P. Bonoli, C. Christensen, C. Fiore, D. Garnier, J. Goetz, S. Golovato, R. Granetz, M. Greenwald, S. Horne, A. Hubbard, I. Hutchinson, J. Irby, B. LaBombard, B. Lipschultz, E. Marmar, M. May, A. Mazurenko, G. Mccracken, P. O'shea, M. Porkolab, J. Reardon, J. Rice, C. Rost, J. Schachter, J. Snipes, P. Stek, J. Terry, R. Watterson, B. Welch, S. Wolfe, Radiofrequency-heated enhanced confinement modes in the Alcator C-Mod tokamak, *Phys. Plasmas* 4 (5) (1997) 1647–1653.
- [31] M. Greenwald, R. Boivin, P. Bonoli, R. Budny, C. Fiore, J. Goetz, R. Granetz, A. Hubbard, I. Hutchinson, J. Irby, B. LaBombard, Y. Lin, B. Lipschultz, E. Marmar, A. Mazurenko, D. Mossessian, T. Sunn Pedersen, C.S. Pitcher, M. Porkolab, J. Rice, W. Rowan, J. Snipes, G. Schilling, Y. Takase, J. Terry, S. Wolfe, J. Weaver, B. Welch, S. Wukitch, Characterization of enhanced Da high-confinement modes in Alcator C-Mod, *Phys. Plasmas* 6 (5) (1999) 1943–1949.
- [32] L. Gil, C. Silva, T. Happel, G. Birkenmeier, G. Conway, L. Guimaraes, A. Kallenbach, T. Pütterich, J. Santos, P. Schneider, M. Schubert, E. Seluin, A. Silva, J. Stober, U. Stroth, E. Trier, E. Wolfrum, the ASDEX Upgrade Team, the EUROfusion MST1 Team, Stationary ELM-free H-mode in ASDEX upgrade, *Nucl. Fusion* 60 (5) (2020) 054003.

- [33] A. Kallenbach, M. Bernert, P. David, M.G. Dunne, R. Dux, E. Fable, R. Fischer, L. Gil, T. Görler, F. Janky, R.M. McDermott, W. Suttrop, G. Tardini, M. Wischmeier, ASDEX Upgrade Team, EUROfusion MST1 team, Developments towards an ELM-free pedestal radiative cooling scenario using noble gas seeding in ASDEX upgrade, *Nucl. Fusion* 61 (1) (2020) 016002.
- [34] D.A. Mossessian, R.J. Groebner, R.A. Moyer, T.H. Osborne, J.W. Hughes, M. Greenwald, A. Hubbard, T.L. Rhodes, Edge dimensionless identity experiment on DIII-D and Alcator C-Mod, *Phys. Plasmas* 10 (3) (2003) 689–698.
- [35] Y. Kamada, R. Yoshino, Y. Neyatani, M. Sato, S. Tokuda, M. Azumi, S. Takeji, K. Ushigusa, T. Fukuda, M. Mori, T. Takizuka, the JT-60U Team, Onset condition for ELMs in JT-60U, *Plasma Phys. Control. Fusion* 38 (8) (1996) 1387.
- [36] R. Nazikian, C. Petty, A. Bortolon, X. Chen, D. Eldon, T. Evans, B. Grierson, N. Ferraro, S. Haskey, M. Knolker, C. Lasnier, N. Logan, R. Moyer, D. Orlov, T. Osborne, C. Paz-Soldan, F. Turco, H. Wang, D. Weisberg, Grassly-ELM regime with edge resonant magnetic perturbations in fully noninductive plasmas in the DIII-D tokamaka, *Nucl. Fusion* 58 (10) (2018) 106010.
- [37] G. Xu, Q. Yang, N. Yan, Y. Wang, X. Xu, H. Guo, R. Maingi, L. Wang, J. Qian, X. Gong, V. Chan, T. Zhang, Q. Zang, Y. Li, L. Zhang, G. Hu, B. Wan, Promising high-confinement regime for steady-state fusion, *Phys. Rev. Lett.* 122 (25) (2019) 255001.
- [38] N. Oyama, P. Gohil, L.D. Horton, A.E. Hubbard, J.W. Hughes, Y. Kamada, K. Kamiya, A.W. Leonard, A. Loarte, R. Maingi, G. Saibene, R. Sartori, J.K. Stober, W. Suttrop, H. Urano, W.P. West, the ITPA Pedestal Topical Group, Pedestal conditions for small ELM regimes in tokamaks, *Plasma Phys. Control. Fusion* 48 (5A) (2006) A171.
- [39] R. Maingi, A. Hubbard, H. Meyer, J. Hughes, A. Kirk, R. Maqueda, J. Terry, Comparison of small ELM characteristics and regimes in Alcator C-Mod, MAST and NSTX, *Nucl. Fusion* 51 (6) (2011) 063036.
- [40] N. Oyama, A. Kojima, N. Aiba, L. Horton, A. Isayama, K. Kamiya, H. Urano, Y. Sakamoto, Y. Kamada, Effects of edge collisionality on ELM characteristics in the grassy ELM regime, *Nucl. Fusion* 50 (6) (2010) 064014.
- [41] T. Eich, P. Manz, the ASDEX Upgrade team, The separatrix operational space of ASDEX Upgrade due to interchange-drift-Alfvén turbulence, *Nucl. Fusion* 61 (8) (2021) 086017.
- [42] B.D. Scott, Drift wave versus interchange turbulence in tokamak geometry: Linear versus nonlinear mode structure, *Phys. Plasmas* 12 (6) (2005) 062314.
- [43] R. Aymar, P. Barabaschi, Y. Shimomura, The ITER design, *Plasma Phys. Control. Fusion* 44 (5) (2002) 519.
- [44] M. Sicciano, J. Graves, R. Kembleton, H. Lux, F. Maviglia, A. Morris, J. Morris, H. Zohm, Development of the plasma scenario for EU-DEMO: Status and plans, *Fusion Eng. Des.* 176 (2022) 113047.
- [45] M. Greenwald, Density limits in toroidal plasmas, *Plasma Phys. Control. Fusion* 44 (8) (2002) R27.
- [46] O. Sauter, C. Angioni, Y.R. Lin-Liu, Neoclassical conductivity and bootstrap current formulas for general axisymmetric equilibria and arbitrary collisionality regime, *Phys. Plasmas* 6 (7) (1999) 2834–2839.
- [47] M.G. Dunne, L. Frassinetti, M.N.A. Beurskens, M. Cavedon, S. Fietz, R. Fischer, L. Giannone, G.T.A. Huijsmans, B. Kurzan, F. Laggner, P.J. McCarthy, R.M. McDermott, G. Tardini, E. Viezzzer, M. Willensdorfer, E. Wolfrum, the ASDEX Upgrade Team, the EUROfusion MST1 Team, Global performance enhancements via pedestal optimisation on ASDEX upgrade, *Plasma Phys. Control. Fusion* 59 (2) (2016) 025010.
- [48] M. Bernert, T. Eich, A. Kallenbach, D. Carralero, A. Huber, P.T. Lang, S. Potzel, F. Reimold, J. Schweinzer, E. Viezzzer, H. Zohm, the ASDEX Upgrade team, The H-mode density limit in the full tungsten ASDEX Upgrade tokamak, *Plasma Phys. Control. Fusion* 57 (1) (2014) 014038.
- [49] A. Huber, M. Bernert, S. Brezinsek, A. Chankin, G. Sergienko, V. Huber, S. Wiesen, P. Abreu, M. Beurskens, A. Boboc, M. Brix, G. Calabro, D. Carralero, E. Delabie, T. Eich, H. Esser, M. Groth, C. Guillemaut, S. Jachmich, A. Järvinen, E. Joffrin, A. Kallenbach, U. Kruezi, P. Lang, C. Linsmeier, C. Lowry, C. Maggi, G. Matthews, A. Meigs, P. Mertens, F. Reimold, J. Schweinzer, G. Sips, M. Stamp, E. Viezzzer, M. Wischmeier, H. Zohm, Comparative H-mode density limit studies in JET and AUG, *Nucl. Mater. Energy* 12 (2017) 100–110, Proceedings of the 22nd International Conference on Plasma Surface Interactions 2016, 22nd PSI.
- [50] P. Manz, T. Eich, O. Grover, the ASDEX Upgrade Team, The power dependence of the maximum achievable H-mode and (disruptive) L-mode separatrix density in ASDEX upgrade, *Nucl. Fusion* 63 (7) (2023) 076026.
- [51] M. Faitsch, I. Balboa, P. Lomas, S. Silburn, A. Tookey, D. Kos, A. Huber, E. de la Luna, D. Keeling, A. Kappatou, JET Contributors, Divertor power load investigations with deuterium and tritium in type-I ELMy H-mode plasmas in JET with the ITER-like wall, *Nucl. Fusion* 63 (11) (2023) 112013.
- [52] T. Eich, R. Goldston, A. Kallenbach, B. Sieglin, H. Sun, ASDEX Upgrade Team, JET Contributors, Correlation of the tokamak H-mode density limit with ballooning stability at the separatrix, *Nucl. Fusion* 58 (3) (2018) 034001.
- [53] T. Eich, A. Leonard, R. Pitts, W. Fundamenski, R. Goldston, T. Gray, A. Herrmann, A. Kirk, A. Kallenbach, O. Kardaun, A. Kukushkin, B. LaBombard, R. Maingi, M. Makowski, A. Scarabosio, B. Sieglin, J. Terry, A. Thornton, ASDEX Upgrade Team, JET EFDA Contributors, Scaling of the tokamak near the scrape-off layer H-mode power width and implications for ITER, *Nucl. Fusion* 53 (9) (2013) 093031.
- [54] C.S. Chang, S. Ku, A. Loarte, V. Parail, F. Köchl, M. Romanelli, R. Maingi, J.-W. Ahn, T. Gray, J. Hughes, B. LaBombard, T. Leonard, M. Makowski, J. Terry, Gyrokinetic projection of the divertor heat-flux width from present tokamaks to ITER, *Nucl. Fusion* 57 (11) (2017) 116023.